ACS APPLIED MATERIALS & INTERFACES

Research Article

www.acsami.org

DNA–Carbon Dots Function as Fluorescent Vehicles for Drug Delivery

Han Ding,[†] Feiyue Du,[†,ϕ] Pengchang Liu,[†,ϕ] Zhijun Chen,*[,†,ϕ] and Jiacong Shen[†]

[†]State Key Laboratory of Supramolecular Structure and Materials and International Joint Research Laboratory of Nano-Micro Architecture Chemistry, Jilin University, 2699 Qianjin Street, 130012 Changchun, P. R. China

[ϕ]Institute of Theoretical Chemistry, Jilin University, 130012 Changchun, P. R. China

Supporting Information

ABSTRACT: Carbon dots (CDs) are a new representative in the carbon-based material family, attracting tremendous interest in a large variety of fields, including biomedicine. In this report, we described a facile and green system for synthesizing DNA–CDs using genomic DNA isolated from *Escherichia coli*. DNA–CDs can be purified using a simple column centrifugation-based system. During DNA–CD synthesis, ribose was collapsed, accompanied by the release of nitrogen, and several new bonds (C–OH, N–O, and N–P) were formed, while the other covalent bonds of DNA were largely maintained. The presence of abundant chemical groups, such as amino or hydroxyl groups on DNA–CDs, may facilitate their future functionalization. These highly biocompatible DNA–CDs can serve as a new type of fluorescent vehicle for cell imaging and drug delivery studies. Our research may hasten the development of CDs for prominent future biomedical applications.

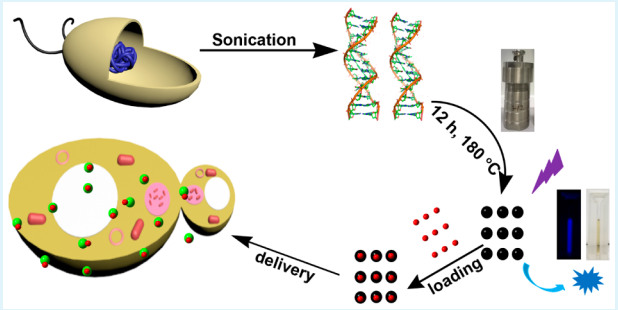

KEYWORDS: *DNA–carbon dots, new bond formation, fluorescent vehicle, drug delivery*

1. INTRODUCTION

Nanomaterials are emerging as a new topic that shows great potential for making a significant impact in the frontiers of biological sciences and clinical and medical research. In particular, various nanomaterials are being used in cell fluorescent imaging and drug delivery applications, providing visual information for cell conditions and disease analysis as well as smart systems for targeted transport of molecules into specific organelles, cells, and organs. Among the advanced nanomaterials, carbon dots (CDs) are a new representative in the carbon-based material family alongside other fluorescent carbon-based nanomaterials, such as carbon nanotubes (CNTs)[1−4] and graphene quantum dots (GQDs).[5,6] Compared to most of the other fluorescent nanomaterials, CDs show good biocompatibility, tunable emission wavelengths, and excellent photostability.[7,8]

Hydrothermal synthesis is one of the most widely used methods for synthesizing CDs. During the hydrothermal synthetic process, dehydrants and/or oxidants are frequently employed, which include H_2O_2,[9,10] H_2SO_4,[11,12] phosphorus pentoxide,[13] and phosphoric acid.[14,15] Similarly, microwaves have also been used for CD synthesis.[15−17] Notably, the characteristics of CDs are partially dependent on the starting raw materials that were used in the hydrothermal synthesis of CDs. These raw materials can be sugars,[14,16] amino acids,[10,15] organic molecules,[18] wasted food,[19] coffee,[20,21] honey from bees,[22] juice,[23−26] proteins,[27] milk,[28] and plastic bags.[9] The synthesized CDs based on these templates showed distinct photophysical and biochemical properties. It is important to find an alternative environmentally friendly route to synthesize highly fluorescent CDs that contain new properties and are suitable for biomedical applications.

The physicochemical characteristics of CDs determine their function and potential use in biomedical studies. To date, many applications of CDs have been studied. First, CDs have shown a capacity for analytical investigations.[7,8,29−31] For instance, CDs can work as sensors for mercury (methyl mercury),[25,32−35] copper,[36−38] zinc,[39] and iron ions,[40−43] and for antibiotic detection.[44,45] Second, CDs can serve as pH responsive materials[11,46,47] or catalysts.[48−50] And finally, although still in its infancy, CDs have shown promise in next generation bioimaging[10,11,14,18,19,26,27,46,51,52] and drug delivery studies.[27,53,54]

In this report, we developed a dehydrant/oxidant-free hydrothermal CD-synthesizing approach by using bacterial genomic DNA as the starting material. These DNA–CDs are highly fluorescent, biocompatible, and can be easily purified using spin-columns. DNA–CDs can be readily internalized by different type of cells and serve as vehicles to deliver dyes and drugs into eukaryotic cells. Therefore, we propose that DNA–CDs may serve as a new platform for bioimaging and drug delivery studies.

Received: January 21, 2015
Accepted: March 5, 2015
Published: March 5, 2015

DOI: 10.1021/acsami.5b00628
ACS Appl. Mater. Interfaces 2015, 7, 6889−6897

2. EXPERIMENTAL SECTION

Chemicals. Chemical compounds, such as yeast extract, trypton, glucose and sucrose, sodium hydroxide (NaOH), hydrochloric acid (HCl), phosphate buffer, sodium chloride (NaCl), Tris-base, and HEPES, were purchased from Beijing Chemical Reagent Company (Beijing, China). Double-distilled water (dH_2O) used in the experiments was obtained from a Milli-Q system (Millipore, Bedford, MA, USA).

Instruments and Characterization. An incubator shaker (IS-RDS3, Crystal, Suzhou, China) and high-speed refrigerated centrifuge (Anhui USTC Shaker Zonkia Scientific Instruments, Hefei, China) were used to mix and separate samples. UV−visible and fluorescence spectra were obtained on a UV-3600 spectrophotometer (Shimadzu, Tokyo, Japan) and a 5301PC spectrophotometer (Shimadzu), respectively. The fluorescence lifetimes of the samples were recorded on an Edinburgh Instruments fls920 spectrofluorometer equipped with continuous (450 W) xenon lamp (Edinburgh, U.K.). An SPA 300 atomic force microscope (AFM, NSK, Japan) was used for size and morphology analysis. X-ray photoelectron spectroscopy (XPS) data were collected on a Kratos AXIS X-ray photoelectron spectrometer (Manchester, U.K.). The valence states and composition of the nanoclusters were collected on a Kratos AXIS X-ray photoelectron spectrometer. The Malvern ZEN 3600 Zetasizer (Malvern Instruments Ltd., U.K.) was used to investigate the synthesized particle sizes and zeta potentials. Microbe fluorescent images were collected using a laser confocal inverted microscope (FV1000, Olympus, Japan). X-ray diffraction (XRD) data were collected on a SmartLab 3 (Rigaku, Tokyo, Japan).

DNA Isolation. *Escherichia coli* genomic DNA isolation was performed according to a protocol by Zhang et al. with modest modifications. Briefly, *E. coli* (DH5α) was inoculated in 1 L of lysogeny broth (LB) media for O/N culture until OD_{600} reached ~3.5. The *E. coli* cells were collected based on a centrifugation system (4000*g*, 20 min). The cell pellets were washed with PBS buffer (pH 7.4) and resuspended using 20 mL of dH_2O. *E. coli* cells were broken using a sonicator (60% intensity, 9.9 s on and 9.9 s off for a total of 6 min) (Noise Isolating Tamber SCIENTZ-IID, Ningbo Scientz Biotechnology Co. Ltd) and centrifuged (2500*g*, 20 min) to remove debris. The supernatant was then collected and incubated in a boiling water bath for 10 min. The resulting mixture was then centrifuged (2500*g*, 20 min), and the pellet was collected and resuspended in dH_2O. The concentration of the DNA was then determined using a spectrophotometer (Eppendorf Biophotometer Plus, Eppendorf China Ltd.) and DNA agarose gel electrophoresis.

Synthesis and Purification of DNA−CDs. DNA (4 mg/mL in dH_2O) was introduced into a hydrothermal synthesis reaction kettle (Gongyi City Yuhua Instrument Co., Ltd., Gongyi, China) with a capacity of 20 mL and incubated at 180 °C in an electric thermostatic drying oven (DGG-9070B, Shanghai SUMSUNG Laboratory Instrument Co., Ltd., Shanghai, China) for 12 h. The resulting DNA−CD-containing mixture was centrifuged at 11000*g* for 30 min. The supernatant was purified using a PCR purification kit (GENOMED GmbH Company, Löhne, Germany), followed by complete dialysis (3500 Da) for 48 h.

Cell Culture and Imaging. *E. coli* and *Saccharomyces cerevisiae* cells were incubated in fresh LB/YPD media until they reached an OD_{600} of 0.5 and 5.0, respectively. The cells were then centrifuged, and the pellets were resuspended using fresh LB/YPD.

DNA−CDs were mixed with the cell-containing media to a final concentration of 0.2 mM. The mixture was incubated at room temperature in a QB-228 rolling incubator (Kylin-Bell Lab Instruments Co. Ltd., Haimen, China) for 6 h. These *E. coli* and/or *S. cerevisiae* cells were then washed three times using PBS buffer (pH 7.4) and subjected to imaging analysis.

For mammalian cell imaging studies, human embryonic kidney (HEK) 293 cells were incubated in DMEM medium supplemented with 10% (v/v) fetal bovine serum (FBS), 100 U/ml penicillin, and 100 mg/mL streptomycin. HEK 293 cells were seeded into each well of a 6-well plate and incubated overnight at 37 °C in a humidified atmosphere supplemented with 5% CO_2. Culture medium was replaced by 400 μL of medium containing either DNA−CD−propidium iodide (PI) complexes (0.2 mM) or PI (0.1 mg/mL) alone and further incubated for 4 h, followed by washing in 1× PBS buffer (pH 7.4) 3 times. Cellular uptake and PI delivery were detected using a high content imaging fluorescent microscope (Operetta from PerkinElmer). The excitation wavelengths used for DNA−CDs and PI were 405 and 535 nm, respectively.

Cytotoxicity Analysis. A colony of *E. coli* DH5α from an LB plate was added to LB media and incubated overnight at 37 °C at 150 rpm until the OD_{600} of the culture reached ~3.5. *E. coli* cells were then collected by centrifugation, washed with PBS buffer (pH 7.4), and resuspended with fresh LB medium to an OD_{600} of ~0.3. DNA−CDs (0.2 mM final concentration) were added to one aliquot of the cells, whereas another aliquot of the cells was mixed with an equal volume of PBS buffer as the control. These cell samples were incubated at 37 °C (150 rpm by shaking) until they reached steady growth (OD_{600} was measured at intervals).

Loading of Dye and/or Drug Molecules. DNA−CDs (0.2 mM) were mixed with either rhodamine 6G (Rh 6G) (0.1 mg/mL), doxorubicin (Dox, 0.1 mg/mL), or PI (0.1 mg/mL) in a neutralized aqueous solution and stirred for 12 h in a dark place. To remove the unbound Rh 6G, Dox, or PI, the resulting mixture was dialyzed (molecular weight cutoff of 3500 Da) against dH_2O for ~48 h until no fluorescent signal could be detected from the solutions outside of the dialysis tubes.

For the drug release test, DNA−CDs−Rh 6G (400 μL) in a dialysis bag was incubated with 3 mL of buffer solution (1× PBS buffer at pH 7.2 or 20 mM HAc-NaAc buffer at pH 4.1) in a cuvette. Rh 6G release with respect to the buffer solutions was monitored by analyzing the absorbance of Rh 6G at 530 nm.

Statistical Analysis. All data in this article were expressed as the mean result ± standard deviation (SD). All figures shown in this article were obtained from three independent experiments with similar results. The statistical analysis was performed using Origin 8.5 software.

3. RESULTS AND DISCUSSION

Recent advances have indicated that the fluorescent properties of CDs are tunable by modulating the content of nitrogen and phosphorus elements within CDs.[18,55] Notably, DNA is a nitrogen and phosphorus-rich polymeric material that is among the most widespread, renewable biomaterials in nature.

Scheme 1. Schematic Representation of DNA−CD Synthesis and Its Application in Bioimaging and Drug Delivery

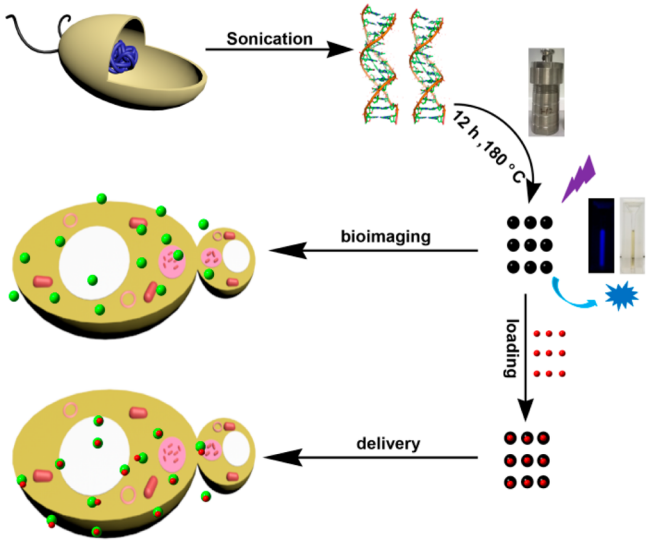

DOI: 10.1021/acsami.5b00628
ACS Appl. Mater. Interfaces 2015, 7, 6889−6897

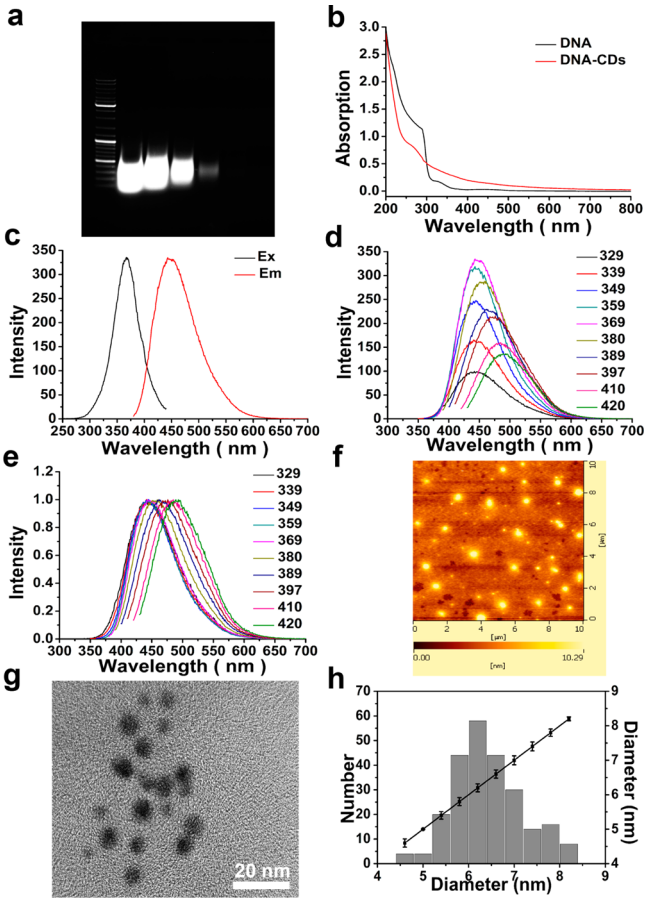

Figure 1. Spectroscopic characterization and spin-column purification of DNA−CDs. (a) Agarose gel electrophoresis of the isolated DNA from *E. coli*. (b) UV−vis absorption spectra of DNA and DNA−CDs. (c) Fluorescence excitation and emission spectra of DNA−CDs. (d) Excitation-dependent emission shift of DNA−CDs. (e) Normalized results of (d). (f and g) Representative AFM (f) and TEM (g) microimages of DNA−CDs. (h) Size distribution of DNA−CDs obtained from TEM analysis.

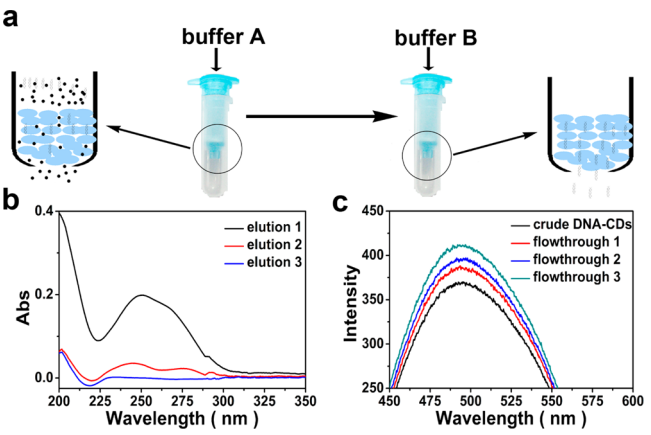

Figure 2. (a) Schematic illustration of DNA−CD purification using DNA-affinity spin columns. (b) UV−vis absorption spectra of eluted fractions from the spin columns. (c) Fluorescence spectra of DNA−CDs before and after purification. 1−3 refer to the number of purification cycles.

However, DNA is very rarely used as a starting material considering its potential for carbon-based material synthesis, particularly with CDs.

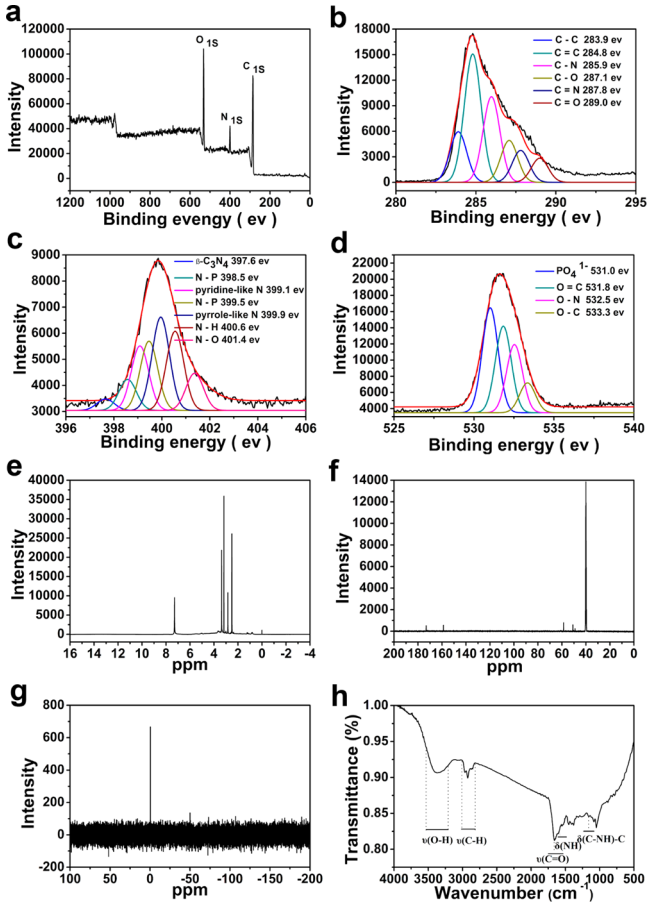

Figure 3. From XPS of the DNA−CDs (a), a speculative mechanism of DNA−CD synthesis was proposed. (b) C1s XPS spectra showed carbon-related covalent bonds within DNA−CDs. (c) N1s XPS spectra showed nitrogen forming covalent bonds. (d) O1s XPS spectra showed oxygen forming covalent bonds. (e) H NMR, (f) C NMR, (g) P NMR, and (h) FTIR spectra of DNA−CDs.

E. coli is a typical laboratory model organism that is widely used in molecular biological and microbiological research. *E. coli* contain a circular genomic DNA in its nuclear zone, which is ∼4.6 million base pairs in length. It is rather easy and cost-effective to manipulate *E. coli* and to isolate genomic DNA from the bacterial cells. Thus, this bacterial system was chosen for our investigation (Scheme 1).

E. coli cells were incubated by shaking in fresh LB medium for 24 h at 37 °C. The cells were collected by centrifugation and washed using phosphate buffer saline (PBS buffer, pH 7.4) 3 times. DNA was extracted from the bacterial cells using a protocol modified from the literature.[56] For a detailed procedure, see the Supporting Information. Briefly, cells were broken using sonication. Contaminants (e.g., proteins and cell membranes) were removed by adjusting the pH, followed by heating in a boiling water bath for 10 min and centrifugation (2500*g*, 20 min). The isolated genomic DNA fragments were diluted to 4 mg/mL and then transferred to a hydrothermal synthesis reaction kettle in an electric thermostatic drying oven and heated for 12 h at 180 °C. The synthesized CDs were centrifuged, spin-column purified, dialyzed against dH_2O, and lyophilized prior to use. Importantly, this approach is free from dehydrant or any other environmental unfriendly compounds, which ensures a high level of biocompatibility.

DOI: 10.1021/acsami.5b00628
ACS Appl. Mater. Interfaces 2015, 7, 6889−6897

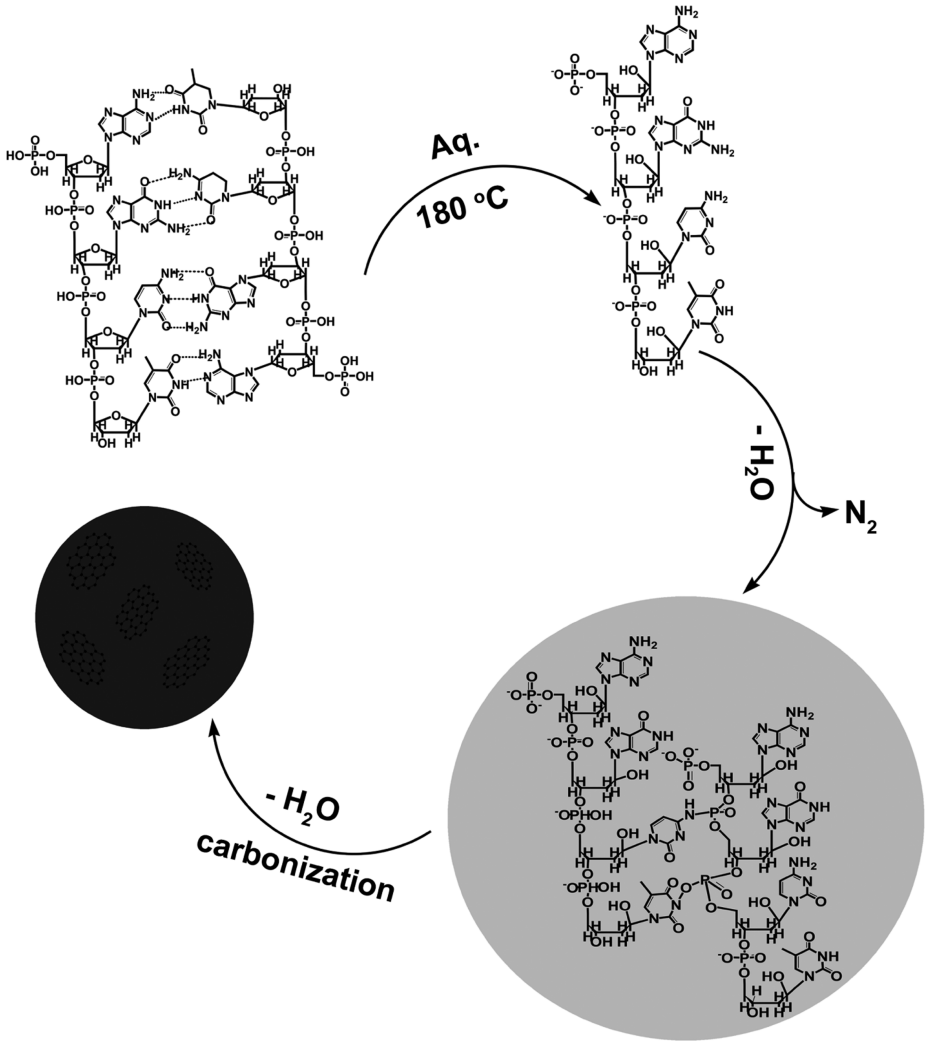

Figure 4. Proposed mechanism for DNA−CD synthesis: denaturation, condensation, polymerization, and carbonization.

Genomic DNA was isolated and purified from *E. coli* cells. Because of the sonication treatment to break the cells, the DNA is fragmented with an average size of ∼300 bp (Figure 1a). Similar to other DNAs, bacterial genomic DNA shows a characteristic UV−vis absorption peak at 280 nm. This peak was diminished when DNA−CDs were formed (Figure 1b). DNA−CDs synthesized using this green approach show excitation and emission peaks at 366 and 445 nm, respectively (Figure 1c). DNA−CDs also show an emission wavelength tunable characteristic that is dependent on the excitation wavelengths upon UV irradiation (Figure 1d and e). The size of the DNA−CDs was ∼6 nm as shown by the results of atomic force microscope (AFM) and transmission electron microscope (TEM) microimage analysis (Figure 1f−h).

To remove unreacted residual DNA within the synthesized DNA−CD mixture, we applied a PCR purification kit containing DNA-affinity spin columns (Figure 2a). The purification protocol was administered according to the instruction manual with small modifications. Specifically, DNA−CDs were diluted with the supplied binding buffer (buffer A) and loaded onto the column. After centrifugation, DNA−CDs were recovered from the flowthrough pool, and the residual DNA still bound to the columns was eluted using elution buffer B. This simple process removed a substantial amount of contaminant DNA as shown by the UV−vis spectra (Figure 2b). The purified DNA−CDs showed fluorescence emission that was enhanced compared to their crude counterparts (Figure 2c).

In contrast to most of the hydrothermally synthesized CDs reported, DNA−CDs are independent of dehydrant/oxidant supply. The synthetic mechanism of DNA−CDs can be investigated using X-ray photoelectron spectroscopy (XPS).[57−66] It was shown that DNA−CDs contain most of the covalent bonds that exist in the natural form of DNA as shown by C1s, N1s, and O1s XPS, H NMR, C NMR, P NMR and Fourier transform infrared spectroscopy (FTIR) spectra (Figure 3a−h, Figure S2 in the Supporting Information). Surprisingly, two new bonds (N−O and N−P) that do not exist in natural DNA were formed within DNA−CDs, as shown by N1s XPS spectra (Figure 3c). C NMR spectra hinted that the ribose ring of DNA may be opened, accompanied by the formation of a C−OH group (Figure 3f). P NMR spectra showed that the phosphate group remains in the DNA−CDs (Figure 3g). Elemental analysis showed that the contents of N, C, and H elements were 8.03%, 51.24%, and 6.09%, respectively, suggesting that the content of the N element was significantly decreased compared to DNA prior to heating. This result suggests that certain NH_2 groups may be released by forming N_2 during the hydrothermal reaction. From these observations, we propose a model speculating the putative mechanism of DNA−CD synthesis: The amino containing

DOI: 10.1021/acsami.5b00628
ACS Appl. Mater. Interfaces 2015, 7, 6889−6897

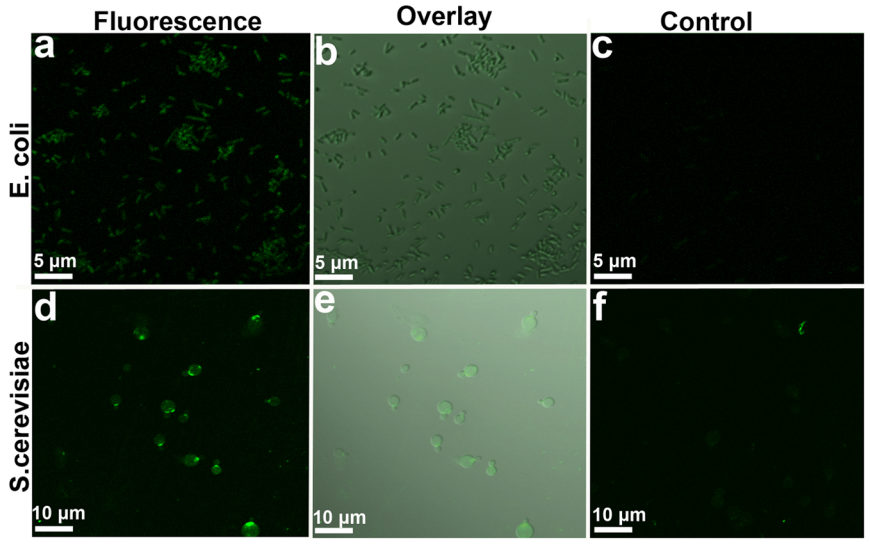

Figure 5. DNA−CDs were readily internalized by bacteria and yeast. DNA−CDs entered (a and b) *E. coli* or (d and e) *S. cerevisiae* cells and emitted green signal upon UV irradiation (405 nm) as shown on CFM images. The overlays (b and e) are merged pictures of the fluorescent and bright field images. No fluorescent signal is detected in (c) *E. coli* or (f) *S. cerevisiae* cells in the absence of CDs.

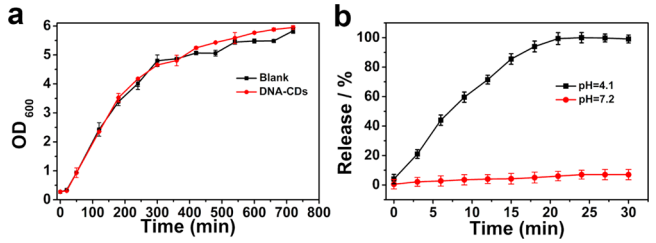

Figure 6. (a) Cytotoxicity evaluation of DNA−CDs and (b) the release profile of Rh 6G from DNA−CDs−Rh 6G complexes at different pH. The growth of *E. coli* cells was not affected by the presence of 0.2 mM DNA−CDs as shown by the optical density (OD) measurement at 600 nm (a). For drug release experiments (b), DNA−CDs−Rh 6G (400 μL) was added to a mini-dialysis bag incubated with test tubes containing 3 mL of buffer (1× PBS buffer at pH 7.2 or 20 mM NaAc buffer at pH 4.1). The release of Rh 6G was monitored at 530 nm by UV−vis spectra (b). The plotted values are the mean ± SD (n = 3).

groups on the nitrogenous bases of DNA (e.g., adenine, thymine, cytosine, and guanine) may interact with neighboring phosphoric acid groups to undergo dehydration, condensation, and carbonization under hydrothermal conditions (Figure 4.) The purified DNA−CDs were further characterized by various techniques (Figures S4−S6 in the Supporting Information), suggesting good physicochemical properties.

The ability of nanomaterials to be readily taken up by cells is an important measure for their possible use in biomedical research, especially for cell imaging and drug delivery studies. Microbes, such as *E. coli* and *S. cerevisiae*, served as models to evaluate their internalization capability toward DNA−CDs. *E. coli* (or *S. cerevisiae*) cells were mixed with DNA−CDs (0.1 mg/mL) in LB (or yeast extract peptone dextrose, YPD) media and incubated for 6 h at 37 °C (or 30 °C). These cell samples were washed 3 times with PBS buffer (pH 7.4) before being subjected to imaging analysis by confocal fluorescence microscopy (CFM). Interestingly, DNA−CDs were easily internalized by either *E. coli* or *S. cerevisiae* cells (Figure 5), suggesting that they may be used in either bacterial or eukaryotic cell related studies.

Notably, DNA−CDs are highly biocompatible as shown by cytotoxicity experiments (Figure 6a). To test the possibility of DNA−CDs serving as vehicles for drug delivery studies, we used rhodamine 6G (Rh 6G) and doxorubicin (Dox) as test molecules loaded into DNA−CD vehicles. The zeta potentials of DNA−CDs, Rh 6G, and Dox were −22.7, 14.1, and 14.5 mV, respectively (Figures S7−9 in the Supporting Information). Rh 6G (or Dox) can thus be loaded onto DNA−CDs by taking advantage of the electrostatic interactions between Rh 6G (or Dox) and DNA−CDs. The supramolecular complexes that were formed (DNA−CDs−Rh 6G or DNA−CDs−Dox) were completely dialyzed against dH_2O to remove excess unbound Rh 6G (or Dox). The supramolecular interaction between vehicle and cargo was rather stable at neutral pH, whereas a lower pH may trigger drug release from the DNA−CDs (Figure 6b). The purified DNA−CDs−Rh 6G (or DNA−CDs−Dox) complexes were incubated with yeast cells (*S. cerevisiae*) for 6 h at 30 °C. The resulting cell mixtures were washed multiple times using PBS buffer (pH 7.4) and then subjected to CFM imaging analysis. As shown in Figure 7a−c, DNA−CDs delivered Rh 6G into yeast cells where the fluorescence of either DNA−CDs or Rh 6G showed an evenly distributed pattern. DNA−CDs also carried Dox into *S. cerevisiae* cells; however, Dox displayed a punctate pattern that differed from that of DNA−CDs (Figure 7d−f), suggesting that Dox was released from the DNA−CD vehicles within the eukaryotic cells.

To further confirm that DNA−CDs can function as vehicles to deliver small molecules (drugs) into cells, we chose propidium iodide (PI) as a test cargo to be loaded onto DNA−CDs by taking advantage of their electrostatic

DOI: 10.1021/acsami.5b00628
ACS Appl. Mater. Interfaces 2015, 7, 6889−6897

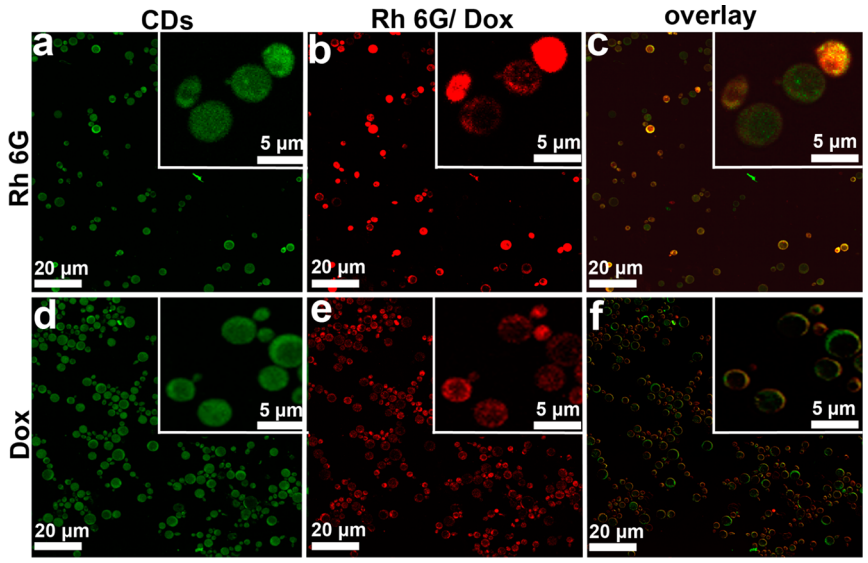

Figure 7. DNA−CDs served as a vehicle for delivering dyes and drugs into *S. cerevisiae* cells. The internalized DNA−CDs and Rh 6G (or Dox) were visualized by blue (a and d) and red channels (b and e) of the CFM, respectively. The overlaid images (c and f) revealed the colocalization of DNA−CDs and Rh 6G, whereas Dox had a distinct punctate distribution, suggesting the release of Dox from the vehicles within the cells. (Insets) Enlarged images.

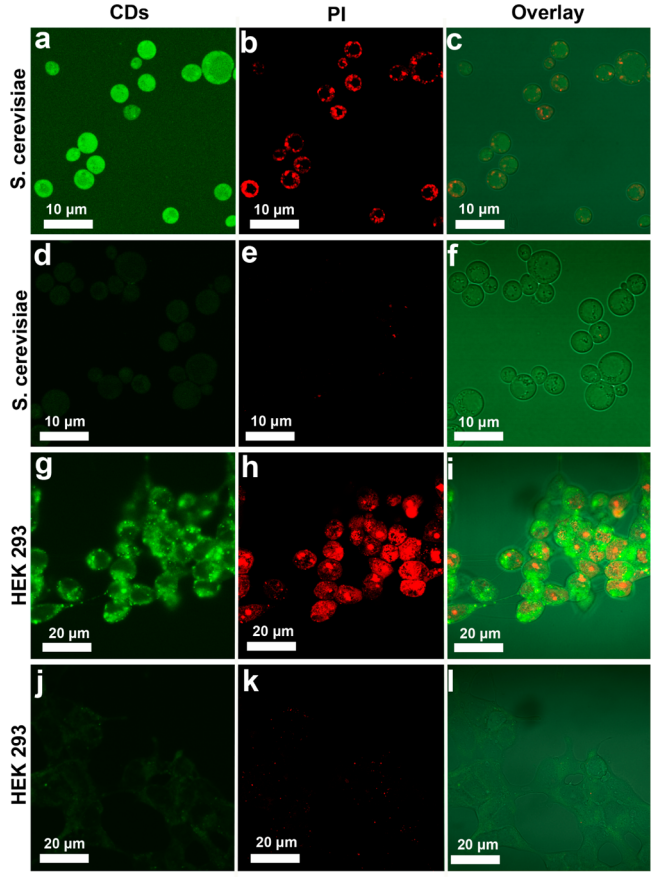

Figure 8. DNA−CDs served as a vehicle for delivering PI into *S. cerevisiae* and HEK 293 cells. The internalized DNA−CDs and PI were visualized by blue (a, d, g, and j) and red channels (b, e, h, and k) of the CFM, respectively. The overlaid images (c, f, i, and l) revealed the partial colocalization of DNA−CDs and PI, suggesting that PI could be partially released from the vehicles within the cells. Notably, PI could enter neither *S. cerevisiae* nor HEK 293 cells by itself, highlighting the vehicle function of DNA−CDs.

interactions. In contrast to Rh 6G and Dox, PI by itself cannot cross the live plasma membrane of eukaryotic cells and thus frequently serves as a marker for dead cell detection. The PI delivery function of DNA−CDs was evaluated using both *S. cerevisiae* and HEK 293 cells (Figure 8). Encouragingly, DNA−CDs not only get through the plasma membrane of

DOI: 10.1021/acsami.5b00628
ACS Appl. Mater. Interfaces 2015, 7, 6889−6897

these cells (Figure 8a and g) but also transport PI into the cells (Figure 8b and h). Notably, barely any PI enters these cells alone, except for the very little amount that might be associated with the cell wall and/or outer membrane (Figure 8e and k). The overlaid images (Figure 8c and i) suggested partial colocalization of DNA−CDs and PI, hinting that PI may be released from the vehicles under some circumstances.

4. CONCLUSIONS

In this report, we developed a facile and green system for synthesizing DNA−CDs using genomic DNA isolated from *E. coli*, which can be easily purified using a simple column centrifugation-based system. A speculative synthetic mechanism of DNA−CDs is presented based on the data obtained from the XPS, NMR, IR, and Elemental analysis, which suggests that the ribose ring may be opened, accompanied by N_2 release, and that two new bonds (N−O and N−P) are formed during the DNA−CD synthesis with the other covalent bonds of DNA being largely maintained within DNA−CDs. The presence of abundant chemical groups, such as amino or hydroxyl groups, on DNA−CDs may facilitate future functionalization studies. Moreover, DNA−CDs can serve as a new platform of fluorescent bioimaging for both prokaryotic and eukaryotic cells and shows promise for delivering drugs into organelles and cells. We expect that our research will hasten the development of CDs for prominent future biomedical applications.

■ ASSOCIATED CONTENT

Supporting Information

XRD, P2p XPS, infrared spectra, fluorescence lifetimes, DNA−CD synthesis at different pH, pH or time-dependent stability of DNA−CDs, and zeta potentials of DNA−CDs, Rh 6G, and Dox. This material is available free of charge via the Internet at http://pubs.acs.org.

■ AUTHOR INFORMATION

Corresponding Author

*E-mail: zchen@jlu.edu.cn. Fax: +86 431-8519-3421. Tel: +86 186-8663-6807.

Funding

This work was supported by the National Natural Science Foundation of China (NSF) (No. 21372097) and a Center of International Mobility (CIMO) grant from Finland.

Notes

The authors declare no competing financial interest.

■ ABBREVIATIONS

XPS, X-ray photoelectron spectroscopy
TEM, transmission electron microscope
SEM, scanning electron microscope
AFM, atomic force microscope
Rh 6G, rhodamine 6G
Dox, doxorubicin

■ REFERENCES

(1) De Volder, M. F. L.; Tawfick, S. H.; Baughman, R. H.; Hart, A. J. Carbon Nanotubes: Present and Future Commercial Applications. *Science* **2013**, *339*, 535−539.
(2) Peng, L. M.; Zhang, Z. Y.; Wang, S. Carbon Nanotube Electronics: Recent Advances. *Mater. Today* **2014**, *17*, 433−442.
(3) Sun, J. Z.; Qin, A. J.; Tang, B. Z. Functional Polyacetylenes: Hybrids with Carbon Nanotubes. *Polym. Chem.* **2013**, *4*, 211−223.
(4) Jia, N. Q.; Lian, Q.; Tian, Z.; Duan, X.; Yin, M.; Jing, L. H.; Chen, S. H.; Shen, H. B.; Gao, M. Y. Decorating Multi-Walled Carbon Nanotubes with Quantum Dots for Construction of Multi-Color Fluorescent Nanoprobes. *Nanotechnology* **2010**, *21*, 1−8.
(5) Lin, L. P.; Rong, M. C.; Luo, F.; Chen, D. M.; Wang, Y. R.; Chen, X. Luminescent Graphene Quantum Dots as New Fluorescent Materials for Environmental and Biological Applications. *TrAC, Trends Anal. Chem.* **2014**, *54*, 83−102.
(6) Zhu, S. J.; Zhang, J. H.; Tang, S. J.; Qiao, C. Y.; Wang, L.; Wang, H. Y.; Liu, X.; Li, B.; Li, Y. F.; Yu, W. L.; Wang, X. F.; Sun, H. C.; Yang, B. Surface Chemistry Routes to Modulate the Photoluminescence of Graphene Quantum Dots: From Fluorescence Mechanism to Up-Conversion Bioimaging Applications. *Adv. Funct. Mater.* **2012**, *22*, 4732−4740.
(7) Song, Y. B.; Zhu, S. J.; Yang, B. Bioimaging Based on Fluorescent Carbon Dots. *RSC Adv.* **2014**, *4*, 27184−27200.
(8) Yang, Z.; Li, Z. H.; Xu, M. H.; Ma, Y. J.; Zhang, J.; Su, Y. J.; Gao, F.; Wei, H.; Zhang, L. Y. Controllable Synthesis of Fluorescent Carbon Dots and Their Detection Application as Nanoprobes. *Nano-Micro Lett.* **2013**, *5*, 247−259.
(9) Hu, Y. P.; Yang, J.; Tian, J. W.; Jia, L.; Yu, J. S. Green and Size-Controllable Synthesis of Photoluminescent Carbon Nanoparticles from Waste Plastic Bags. *RSC Adv.* **2014**, *4*, 47169−47176.
(10) Wei, W. L.; Xu, C.; Wu, L.; Wang, J. S.; Ren, J. S.; Qu, X. G. Non-Enzymatic-Browning-Reaction: A Versatile Route for Production of Nitrogen-Doped Carbon Dots with Tunable Multicolor Luminescent Display. *Sci. Rep.* **2014**, *4*, 1−7.
(11) Hu, Y. P.; Yang, J.; Tian, J. W.; Jia, L.; Yu, J. S. Waste Frying Oil as A Precursor for One-Step Synthesis of Sulfur-Doped Carbon Dots with pH-Sensitive Photoluminescence. *Carbon* **2014**, *77*, 775−782.
(12) Sun, D.; Ban, R.; Zhang, P. H.; Wu, G. H.; Zhang, J. R.; Zhu, J. J. Hair Fiber as a Precursor for Synthesizing of Sulfur-and Nitrogen-Co-Doped Carbon Dots with Tunable Luminescence Properties. *Carbon* **2013**, *64*, 424−434.
(13) Gorakh, B. D.; Kumar, S. S.; Malika, T. K.; Sabyasachi, S. P_2O_5 Assisted Green Synthesis of Multicolor Fluorescent Water Soluble Carbon Dots. *J. Nanosci. Nanotechnol.* **2014**, *14*, 2334−2342.
(14) Xu, Z. Q.; Yang, L. Y.; Fan, X. Y.; Jin, J. C.; Mei, J.; Peng, W.; Jiang, F. L.; Xiao, Q.; Liu, Y. Low Temperature Synthesis of Highly Stable Phosphate Functionalized Two Color Carbon Nanodots and Their Application in Cell Imaging. *Carbon* **2014**, *66*, 351−360.
(15) Jiang, J.; He, Y.; Li, S. Y.; Cui, H. Amino Acids as the Source for Producing Carbon Nanodots: Microwave Assisted One-Step Synthesis, Intrinsic Photoluminescence Property and Intense Chemiluminescence Enhancement. *Chem. Commun.* **2012**, *48*, 9634−9636.
(16) Stefanakis, D.; Philippidis, A.; Sygellou, L.; Filippidis, G.; Ghanotakis, D.; Anglos, D. Synthesis of Fluorescent Carbon Dots by a Microwave Heating Process: Structural Characterization and Cell Imaging Applications. *J. Nanopart. Res.* **2014**, *16*, 2646.
(17) Wang, X. H.; Qu, K. G.; Xu, B. L.; Ren, J. S.; Qu, X. G. Microwave Assisted One-Step Green Synthesis of Cell-Permeable Multicolor Photoluminescent Carbon Dots Without Surface Passivation Reagents. *J. Mater. Chem.* **2011**, *21*, 2445−2450.
(18) Zhu, S. J.; Meng, Q. N.; Wang, L.; Zhang, J. H.; Song, Y. B.; Jin, H.; Zhang, K.; Sun, H. C.; Wang, H. Y.; Yang, B. Highly Photoluminescent Carbon Dots for Multicolor Patterning, Sensors, and Bioimaging. *Angew. Chem., Int. Ed.* **2013**, *125*, 4045−4049.
(19) Park, S. Y.; Lee, H. U.; Park, E. S.; Lee, S. C.; Lee, J. W.; Jeong, S. W.; Kim, C. H.; Lee, Y. C.; Huh, Y. S.; Lee, J. Photoluminescent Green Carbon Nanodots from Food-Waste-Derived Sources: Large-Scale Synthesis, Properties, and Biomedical Applications. *ACS. Appl. Mater. Interfaces* **2014**, *6*, 3365−3370.
(20) Jiang, C. K.; Wu, H.; Song, X. J.; Ma, X. J.; Wang, J. H.; Tan, M. Q. Presence of Photoluminescent Carbon Dots in Nescafe Original Instant Coffee: Applications to Bioimaging. *Talanta* **2014**, *127*, 68−74.
(21) Hsu, P. C.; Shih, Z. Y.; Lee, C. H.; Chang, H. T. Synthesis and Analytical Applications of Photoluminescent Carbon Nanodots. *Green Chem.* **2012**, *14*, 917−920.

DOI: 10.1021/acsami.5b00628
ACS Appl. Mater. Interfaces 2015, 7, 6889−6897

(22) Yang, X. M.; Zhuo, Y.; Zhu, S. S.; Luo, Y. W.; Feng, Y. J.; Dou, Y. Novel and Green Synthesis of High-Fluorescent Carbon Dots Originated from Honey for Sensing and Imaging. *Biosens. Bioelectron.* **2014**, *60*, 292−298.
(23) Sahu, S.; Behera, B.; Maiti, T. K.; Mohapatra, S. Simple One-Step Synthesis of Highly Luminescent Carbon Dots from Orange Juice: Application as Excellent Bio-imaging Agents. *Chem. Commun.* **2012**, *48*, 8835−8837.
(24) De, B.; Karak, N. A Green and Facile Approach for the Synthesis of Water Soluble Fluorescent Carbon Dots from Banana Juice. *RSC Adv.* **2013**, *3*, 8286−8290.
(25) Xu, Y.; Tang, C. J.; Huang, H.; Sun, C. Q.; Zhang, Y. K.; Ye, Q. F.; Wang, A. J. Green Synthesis of Fluorescent Carbon Quantum Dots for Detection of Hg^{2+}. *Chin. J. Anal. Chem.* **2014**, *42*, 1252−1258.
(26) Mehta, V. N.; Jha, S.; Kailasa, S. K. One-Pot Green Synthesis of Carbon Dots by Using Saccharum Officinarum Juice for Fluorescent Imaging of Bacteria (*Escherichia coli*) and Yeast (*Saccharomyces cerevisiae*) Cells. *Mater. Sci. Eng., C* **2014**, *38*, 20−27.
(27) Wang, Q. L.; Huang, X. X.; Long, Y. J.; Wang, X. L.; Zhang, H. J.; Zhu, R.; Liang, L. P.; Teng, P.; Zheng, H. Z. Hollow Luminescent Carbon Dots for Drug Delivery. *Carbon* **2013**, *59*, 192−199.
(28) Wang, L.; Zhou, H. S. Green Synthesis of Luminescent Nitrogen-Doped Carbon Dots from Milk and Its Imaging Application. *Anal. Chem.* **2014**, *86*, 8902−8905.
(29) Hola, K.; Zhang, Y.; Wang, Y.; Giannelis, E. P.; Zboril, R.; Rogachb, A. L. Carbon Dots—Emerging Light Emitters for Bioimaging, Cancer Therapy and Optoelectronics. *Nano Today* **2014**, *402*, 1−14.
(30) Shi, H. T.; Wei, J. F.; Qiang, L.; Chen, X.; Meng, X. W. Fluorescent Carbon Dots for Bioimaging and Biosensing Applications. *J. Biomed. Nanotechnol.* **2014**, *10*, 2677−2699.
(31) Wang, W.; Cheng, L.; Liu, W. G. Biological Applications of Carbon Dots. *Sci. China: Chem.* **2014**, *57*, 522−539.
(32) Guo, Y. M.; Wang, Z.; Shao, H. W.; Jiang, X. Y. Hydrothermal Synthesis of Highly Fluorescent Carbon Nanoparticles from Sodium Citrate and Their Use for the Detection of Mercury Ions. *Carbon* **2013**, *52*, 583−589.
(33) Wang, W. P.; Lu, Y. C.; Huang, H.; Wang, A. J.; Chen, J. R.; Feng, J. J. Solvent-Free Synthesis of Sulfur- and Nitrogen-Co-Doped Fluorescent Carbon Nanoparticles from Glutathione for Highly Selective and Sensitive Detection of Mercury(II) Ions. *Sens. Actuators, B* **2014**, *202*, 741−747.
(34) Zhang, R. Z.; Chen, W. Nitrogen-Doped Carbon Quantum Dots: Facile Synthesis and Application as a "Turn-off" Fluorescent Probe for Detection of Hg^{2+} Ions. *Biosens. Bioelectron.* **2014**, *55*, 83−90.
(35) Isabel, C. M.; Vanesa, R.; Isela, L.; Carlos, B. In Situ Building of a Nanoprobe Based on Fluorescent Carbon Dots for Methylmercury Detection. *Anal. Chem.* **2014**, *86*, 4536−4543.
(36) Sha, Y. F.; Lou, J. Y.; Bai, S. Z.; Wu, D.; Liu, B. Z.; Ling, Y. Hydrothermal Synthesis of Nitrogen-Containing Carbon Nanodots as the High-Efficient Sensor for Copper(II) Ions. *Mater. Res. Bull.* **2013**, *48*, 1728−1731.
(37) Liu, Y. S.; Zhao, Y. N.; Zhang, Y. Y. One-Step Green Synthesized Fluorescent Carbon Nanodots from Bamboo Leaves for Copper (II) Ion Detection. *Sens. Actuators, B* **2014**, *196*, 647−652.
(38) Liu, J. M.; Lin, L. P.; Wang, X. X.; Lin, S. Q.; Cai, W. L.; Zhang, L. H.; Zheng, Z. Y. Highly Selective and Sensitive Detection of Cu^{2+} with Lysine Enhancing Bovine Serum Albumin Modified-Carbon Dots Fluorescent Probe. *Analyst* **2012**, *137*, 2637−2642.
(39) Zhang, Z. M.; Shi, Y. P.; Pan, Y.; Cheng, X.; Zhang, L. L.; Chen, J. Y.; Li, M. J.; Yi, C. Q. Quinoline Derivative-Functionalized Carbon Dots as a Fluorescent Nanosensor for Sensing and Intracellular Imaging of Zn^{2+}. *J. Mater. Chem. B* **2014**, *2*, 5020−5027.
(40) Zhang, P. J.; Xue, Z. J.; Luo, D.; Yu, W.; Guo, Z. H.; Wang, T. Dual-Peak Electrogenerated Chemiluminescence of Carbon Dots for Iron Ions Detection. *Anal. Chem.* **2014**, *86*, 5620−5623.
(41) Yan, X.; Chen, J. L.; Su, M. X.; Yan, F.; Li, B.; Di, B. Phosphate-Containing Metabolites Switch on Phosphorescence of Ferric Ion Engineered Carbon Dots in Aqueous Solution. *RSC Adv.* **2014**, *4*, 22318−22323.
(42) Qu, K. G.; Wang, J. S.; Ren, J. S.; Qu, X. G. Carbon Dots Prepared by Hydrothermal Treatment of Dopamine as an Effective Fluorescent Sensing Platform for the Label-Free Detection of Iron(III) Ions and Dopamine. *Chem.−Eur. J.* **2013**, *19*, 7243−7249.
(43) Song, Y. B.; Zhu, S. J.; Xiang, S. Y.; Zhao, X. H.; Zhang, J. H.; Zhang, H.; Fu, Y.; Yang, B. Investigation into the Fluorescence Quenching Behaviors and Applications of Carbon Dots. *Nanoscale* **2014**, *6*, 4676−4682.
(44) Yang, X. M.; Luo, Y. W.; Zhu, S. S.; Feng, Y. J.; Zhuo, Y.; Dou, Y. One-Pot Synthesis of High Fluorescent Carbon Nanoparticles and Their Applications as Probes for Detection of Tetracyclines. *Biosens. Bioelectron.* **2014**, *56*, 6−11.
(45) Hou, J.; Yan, J.; Zhao, Q.; Li, Y.; Ding, H.; Ding, L. A Novel One-Pot Route for Large-Scale Preparation of Highly Photo-luminescent Carbon Quantum Dots Powders. *Nanoscale* **2013**, *5*, 9558−9561.
(46) Nie, H.; Li, M. J.; Li, Q. S.; Liang, S. J.; Tan, Y. Y.; Sheng, L.; Shi, W.; Zhang, S. X. A. Carbon Dots with Continuously Tunable Full-Color Emission and Their Application in Ratiometric pH Sensing. *Chem. Mater.* **2014**, *26*, 3104−3112.
(47) Jia, X. F.; Li, J.; Wang, E. K. One-Pot Green Synthesis of Optically pH-Sensitive Carbon Dots with Upconversion Lumines-cence. *Nanoscale* **2012**, *4*, 5572−5575.
(48) Li, H. T.; He, X. D.; Kang, Z. H.; Huang, H.; Liu, Y.; Liu, J. L.; Lian, S. Y.; Tsang, C. H. A.; Yang, X. B.; Lee, S. T. Water-Soluble Fluorescent Carbon Quantum Dots and Photocatalyst Design. *Angew. Chem., Int. Ed.* **2010**, *49*, 4430−4434.
(49) Liu, S.; Tian, J. Q.; Wang, L.; Luo, Y. L.; Sun, X. P. A General Strategy for the Production of Photoluminescent Carbon Nitride Dots from Organic Amines and Their Application as Novel Peroxidase-Like Catalysts for Colorimetric Detection of H_2O_2 and Glucose. *RSC Adv.* **2012**, *2*, 411−413.
(50) Ma, Z.; Ming, H.; Huang, H.; Liu, Y.; Kang, Z. H. One-Step Ultrasonic Synthesis of Fluorescent N-Doped Carbon Dots from Glucose and Their Visible-Light Sensitive Photocatalytic Ability. *New J. Chem.* **2012**, *36*, 861−864.
(51) Puvvada, N.; Kumar, B. N. P.; Konar, S.; Kalita, H.; Mandal, M.; Pathak, A. Synthesis of Biocompatible Multicolor Luminescent Carbon Dots for Bioimaging Applications. *Sci. Technol. Adv. Mater.* **2012**, *13*, 1−8.
(52) Sun, Y. P.; Zhou, B.; Lin, Y.; Wang, W.; Fernando, K. A. S.; Pathak, P.; Meziani, M. J.; Harruff, B. A.; Wang, X.; Wang, H. F.; Luo, P. J. G.; Yang, H.; Kose, M. E.; Chen, B. L.; Veca, L. M.; Xie, S. Y. Quantum-Sized Carbon Dots for Bright and Colorful Photo-luminescence. *J. Am. Chem. Soc.* **2006**, *128*, 7756−7757.
(53) Mewada, A.; Pandey, Su.; Thakur, M.; Jadhava, D.; Sharon, M. Swarming Carbon Dots for Folic Acid Mediated Delivery of Doxorubicin and Biological Imaging. *J. Mater. Chem. B* **2014**, *2*, 698−705.
(54) Guo, C. X.; Xie, J.; Wang, B.; Zheng, X.; Yang, H. B.; Li, C. M. A New Class of Fluorescent Dots: Long Luminescent Lifetime Bio-Dots Self-Assembled from DNA at Low Temperatures. *Sci. Rep.* **2013**, *3*, 1−6.
(55) Chen, X. X.; Jin, Q. Q.; Wu, L. Z.; Tung, C. H.; Tang, X. J. Synthesis and Unique Photoluminescence Properties of Nitrogen-Rich Quantum Dots and Their Applications. *Angew. Chem., Int. Ed.* **2014**, *53*, 12542−12547.
(56) Zhang, L.; Foxman, B.; Gilsdorf, J. R.; Marrs, C. F. Bacterial Genomic DNA Isolation Using Sonication for Microarray Analysis. *BioTechniques* **2005**, *39*, 640−644.
(57) Olivares, O.; Likhanova, N. V.; Gómeza, B.; Navarretea, J.; Serranoa, M. E. L.; Arceb, E.; Hallen, J. M. Electrochemical and XPS Studies of Decylamides of α-Amino Acids Adsorption on Carbon Steel in Acidic Environment. *Appl. Surf. Sci.* **2006**, *252*, 2894−2909.
(58) Lewin, E.; Persson, P. O. Å.; Lattemann, M.; Stüber, M.; Gorgoi, M.; Sandell, A.; Ziebert, C.; Schäfers, F.; Braun, W.; Halbritter, J.; Ulrich, S.; Eberhardt, W.; Hultman, L.; Siegbahn, H.; Svenssond, S.;

DOI: 10.1021/acsami.5b00628
ACS Appl. Mater. Interfaces 2015, 7, 6889−6897

Jansson, U. On the Origin of a Third Spectral Component of C1s XPS-Spectra for nc-TiC/aC Nanocomposite Thin Films. *Surf. Coat. Technol.* **2008**, *202*, 3563−3570.
(59) Sobon, G.; Sotor, J.; agiello, J.; Kozinski, J. R.; Zdrojek, M.; Holdynski, M.; Paletko, P.; Boguslawski, J.; Lipinska, L.; Abramski, K. M. Graphene Oxide vs. Reduced Graphene Oxide as Saturable Absorbers for Er-Doped Passively Mode-Locked Fiber Laser. *Opt. Express* **2012**, *20*, 19463−19473.
(60) Bubert, H.; Lambert, J.; Burba, P. Structural and Elemental Investigations of Isolated Aquatic Humic Substances Using X-ray Photoelectron Spectroscopy. *Fresenius' J. Anal. Chem.* **2000**, *368*, 274−280.
(61) Wang, T. S.; Yu, D. L.; Tian, Y. J.; Xiao, F. R.; He, J. L.; Li, D. C.; Wang, W. K.; Li, L. Cubic-C_3N_4 Nanoparticles Synthesized in CN_x/TiN_x Multilayer Films. *Chem. Phys. Lett.* **2001**, *334*, 7−11.
(62) Chowdhury, A. K. M. S.; Cameron, D. C.; Hashmi, M. S. Bonding Structure in Carbon Nitride Films: Variation with Nitrogen Content and Annealing Temperature. *Surf. Coat. Technol.* **1999**, *112*, 133−139.
(63) Jin, C.; Nagaiah, T. C.; Xia, W.; Spliethoff, B.; Wang, S. S.; Bron, M.; Schuhmann, W.; Muhler, M. Metal-Free and Electrocatalytically Active Nitrogen-Doped Carbon Nanotubes Synthesized by Coating with Polyaniline. *Nanoscale* **2010**, *2*, 981−987.
(64) Vassileva, P.; Krastev, V.; Lakov, L.; Peshev, O. XPS Determination of the Binding Energies of Phosphorus and Nitrogen in Phosphazenes. *J. Mater. Sci.* **2004**, *39*, 3201−3202.
(65) Bideux, L.; Metidji, Y. O.; Gruzza, B.; Matolin, V. Study of InP (100) Surface Nitridation by X-ray Photoelectron Spectroscopy. *Surf. Interface Anal.* **2002**, *34*, 712−715.
(66) Majumder, S.; Priyadarshini, M.; Subudhi, U.; Chainy, G. B. N.; Varma, S. X-ray Photoelectron Spectroscopic Investigations of Modifications in Plasmid DNA after Interaction with Hg Nanoparticles. *Appl. Surf. Sci.* **2009**, *256*, 438−442.

DOI: 10.1021/acsami.5b00628
ACS Appl. Mater. Interfaces 2015, 7, 6889−6897